Safety of Nanoparticles: Emphasis on Antimicrobial Properties

17

Kuljit Singh, Shimona Ahlawat, Diksha Kumari, Uma Matlani, Meenakshi, Tejinder Kaur, and Alka Rao

17.1 Introduction

Nanotechnology is the branch of science (nanoscience) that deals with manipulating and tailoring nanosized particles for the desired applicability. The building block of nanotechnology is the nanoparticles (NPs), and this new innovative technology offers an edge over conventional diagnostics and therapeutic approaches (Yetisgin et al. 2020). The properties such as optimal shape, size, larger surface area, biodegradability, biocompatibility, and immune-compatibility make nanomaterials attractive to researchers (Gurunathan et al. 2020). This technology has enabled better bioimaging and improved diagnostic devices, which have further increased therapy success rates in the medical field (Ibrahim 2020). Nanotechnology in agricultural industries has potential applications in crop production, crop improvement, assurance of healthy food, pathogen identification, and removal (Ghorbanpour et al.

K. Singh (✉) · D. Kumari
Infectious Diseases Division, CSIR-Indian Institute of Integrative Medicine, Jammu, India

Academy of Scientific and Innovation Research (AcSIR), Ghaziabad, India
e-mail: singh.kuljit@iiim.res.in

S. Ahlawat · A. Rao (✉)
Academy of Scientific and Innovation Research (AcSIR), Ghaziabad, India

CSIR-Institute of Microbial Technology, Chandigarh, India
e-mail: raoalka@imtech.res.in

U. Matlani · T. Kaur
CSIR-Institute of Microbial Technology, Chandigarh, India

Meenakshi
Academy of Scientific and Innovation Research (AcSIR), Ghaziabad, India

P. V. Mohanan, S. Kappalli (eds.), *Biomedical Applications and Toxicity of Nanomaterials*, https://doi.org/10.1007/978-981-19-7834-0_17

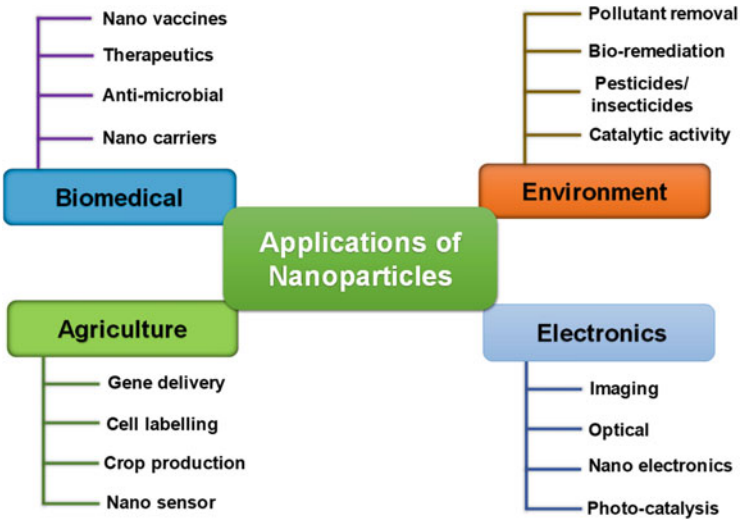

Fig. 17.1 Various applications of nanotechnology

2020). Invention like "Nanosensors" can detect and measure the material derived from bacterial growth and metabolism. Thus, nanosensors can check bacterial and viral toxicity at extremely low concentrations (Rahmati et al. 2020; Kumar et al. 2020). Nanotechnology can also provide solutions for a clean and green environment. A nano fabric towel can absorb 20 times its weight in oil utilized for clean-up purposes (Jin et al. 2018). The use of water-repellent magnetic NPs in oil spills can remove the oil from the water mechanically. Nanotechnology promises an efficient and cost-effective waste-water treatment and thus can help cope with the ever-increasing water demands in the human population. Graphene oxide NPs are increasingly used to filter out air pollutants and purify the air. New NPs-based catalyst has the efficiency to minimize the effect of air pollutants from industrial plants and automobiles (Skinder and Hamid 2020).

NPs are useful in cosmetics, paints, automobiles, space science, and sports utilities. The use of NPs in textiles and fabrics makes them stain resistant, increases sustainability, enhances the quality of food packaging material, and increases the food preservation period, accordingly (Thangadurai et al. 2020). An overview of various applications of nanotechnology is shown in Fig. 17.1. The antimicrobial properties of NPs are of particular interest to researchers. The characteristic of NPs to restrict the growth and metabolism of microbes better than their macroscale counterparts has proved advantageous to overcome the multidrug-resistant mechanism (Wang et al. 2020). For example, cerium oxide NPs cause oxidative stress to eliminate microorganisms (Farias et al. 2018). NPs can serve as antibacterial, antifungal, and antiviral agents (Gudkov et al. 2021; Chen and Liang 2020; Mba and Nweze 2020) both in metallic and biogenic forms (Saleem et al. 2019; Bagchi

and Chauhan 2018). This chapter, in particular, elaborates on the current understanding of NP-based technology for its use as antimicrobial agent.

17.2 Nanoparticles: An Overview

According to the international organization for standardization (ISO), NPs are defined as nano entities that have all three dimensions (3D) in the nanoscale (Sudha et al. 2016). NPs can be formed of several elements, primarily metals, polymers, metal oxides, ceramics, and organic molecules, having salient features that make them desirable for various industrial and pharmaceutical applications (Gharpure et al. 2020). These can be synthesized by chemical processes or environment-friendly methods such as microbes, enzymes, and plants (Hasan 2014). The best-explored applications of NPs include early diagnosis, treatment, and cure of diseases such as cancer, diabetes, and cardiovascular diseases.

17.2.1 Nanoparticles as Drug Carriers

The traditional drug delivery system possesses various constraints such as insolubility of drug, low permeability to the plasma membrane, high dosage of injections, and adverse side effects. The nanotechnology-based drug delivery approach is a novel and emerging concept to overcome the pitfalls of conventional drug delivery approaches (Patra et al. 2018). One can encapsulate the drugs in the internal cavity of the NPs through non-covalent interactions and accomplish the administration of such nanomaterials-based drugs passively. After reaching its target position, the encapsulated structure unfolds, releasing the desired drug to the absolute target. Alternatively, in the self-delivery method, the drug is directly conjugated to the nanocarrier. For target drug delivery, special consideration is necessary during the early drug designing process itself. The coupling between the drug and the carrier NPs is crucial. It has to ensure that the drug does not dissociate too early from the nanocarrier, or else it will be cleared from the body without reaching its required destination. Also, if the drug is not cleaved from its nanocarrier at the optimum time, it will reduce its biological efficacy significantly (Lu et al. 2016). The following section describes the different forms of nanocarriers used for drug delivery with pictorial representation shown in Fig. 17.2.

17.2.1.1 Chitosan

It is a biopolymer extracted from the chitinous shells of sea crustaceans. It is a nontoxic, stable, non-immunogenic, biodegradable polymer employed for the drug delivery process (Ahmad et al. 2021).

17.2.1.2 Alginate

It is a natural polysaccharide derived from the cell walls or intracellular compartments of brown algae, namely *Ascophyllum nodosum* and *Laminaria*

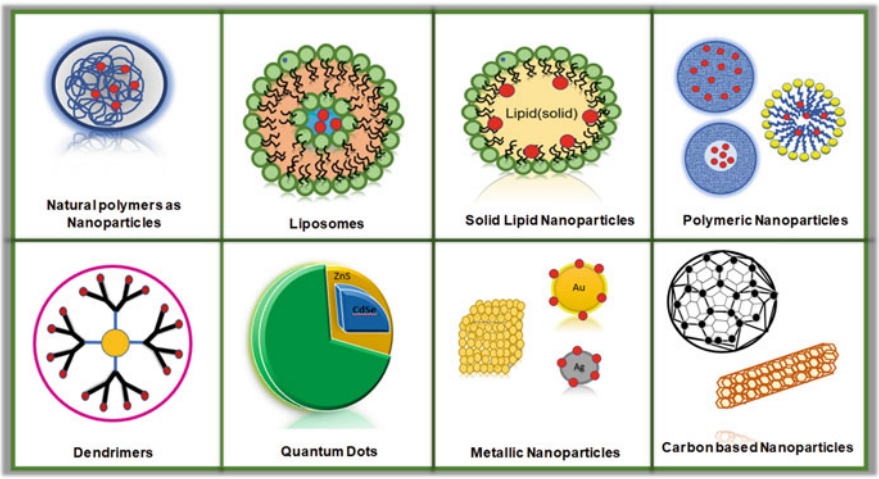

Fig. 17.2 Various forms of nanoparticles used for drug delivery purposes

digitata. With excellent stability, biocompatibility, biodegradability, and reduced toxicity, alginate is a proven agent for various pharmaceutical applications (Hariyadi and Islam 2020).

17.2.1.3 Liposomes

These are the spherical vesicles consisting of an inner aqueous core encapsulated around a phospholipid bilayer. Both water-loving (hydrophilic) and water-repelling (hydrophobic) drugs can form liposomes. Due to their structural similarity with the cell membrane phospholipids and superior pharmacokinetics, liposomes are attractive drug delivery tools in therapeutics (Xing et al. 2016). Apart from making the compound more stable, liposomes fulfill the 3Bs—biodegradable, biocompatible, and biodistribution. However, they are costly to produce (Yadav et al. 2017).

17.2.1.4 Solid Lipid Nanoparticles

As a substitute to conventional carrier systems, namely liposomes, emulsification, and polymeric NPs, solid lipid NPs are another form of nanocarriers for precise drug administration, non-degenerative, and a budget-friendly approach. It consists of a solid lipid matrix, a surfactant such as an emulsifier, a co-surfactant such as water or solvent, and active ingredients, particularly drugs (Basha et al. 2020). Formulations of solid lipid NPs are possible for oral, dermal, and parenteral administration.

17.2.1.5 Polymeric Nanoparticles

The 10–100 nm diametric amphiphilic solid colloidal particles formed of block copolymers hydrophobic core containing hydrophobic drug and water-soluble hydrophilic shell balancing the core are called polymeric nanoparticles. The use of polymeric nanocarriers reduces cytotoxicity and improves the stability and solubility of the drug in the bloodstream. While chitosan and dextran are natural polymers,

polyamide, polyesters, and polyphosphazene are synthetic polymers (Lu et al. 2016). Polymeric micelles have a core and a shell that are hydrophilic. The hydrophilic drug is loaded in the core region of micelles.

Similarly, polymeric nanovesicles have an aqueous core and amphiphilic shell. Thus, nanovesicles can integrate both hydrophobic and hydrophilic materials like proteins, genes, and drugs. However, these structures dissociate into the linear form below its critical micelle concentration; therefore, the nanogel—a more stable polymeric nanoparticle form—is in better demand (Lu et al. 2016).

17.2.1.6 Dendrimers

The term is derived from two Greek words, "dendron" and "meros," which means trees and the parts, respectively (Heera and Shanmugam 2015). Dendrimers indeed are highly branched nanostructures widely used for cancer treatment and bioimaging. With the properties like symmetrical molecular structure and numerous functional groups that can be modified desirably, this becomes a useful candidate for various therapeutics and drug delivery (Abbasi et al. 2014). However, the positively charged dendrimers can alter the cellular membranes and become poisonous to the cell.

17.2.1.7 Quantum Dots

Quantum dots are mini beads of free electrons possessing unique electronic and optical properties. It is a luminescent semiconductor nanocrystal with a 2–10 nm nano-diametric range (Cartaxo 2016). They are generally of two types: simple or core quantum dots (composed of a single material) and core-shell quantum dots (in which the material with a wider energy gap is enclosed by a material having a smaller energy gap). The commonly used material for quantum dots are indium phosphide, cadmium selenide, cadmium telluride, zinc sulfide, and indium arsenide (Ilaiyaraja et al. 2018). These tiny devices are reportable therefore suitable for therapeutic, biosensing, bioimaging, and protein-specific applications or targeting (Riyaz et al. 2019).

17.2.1.8 Metallic Nanoparticles

Metallic NPs consist of metals such as silver, titanium, and gold, metal oxides such as ZnO, magnetic oxides, and semiconductors such as CdS. These are easily transported to the cells due to their appropriate size (10–100 nm) and are not affected by the in vivo environment (Ojea-Jimenez et al. 2013). They are efficient in drug delivery and possess antioxidant properties (Khiev et al. 2021).

17.2.1.9 Carbon-Based Nanoparticles

The different allotropic forms of Carbon are helpful for pharmaceutical applications. Carbon-based NPs include carbon nanotubes, fullerene, and nanodiamonds. Fullerene is a highly symmetrical icosahedron having 60 carbons. Carbon nanotubes are single-walled or multi-walled nanotubes. These have a wide range of applications as they exhibit unique properties, namely elasticity, rigidity, electric conductivity, and thermal conductivity (Wilczewska et al. 2012).

17.2.2 Advantages of Drug Administration Employing Nanoscience

Nanostructure-mediated drug delivery comes with increased solubility, more surface area, high dissociation rates, decreased dosage amount reducing toxicity, improved stability, and many more benefits. Nanoparticle-based therapeutics exhibit better efficiency and site-specific drug release due to their nano size and bioavailability to specific tissue/organs. Also, it reduces the side effects of various drugs (Pardhiya and Paulraj 2016). It prolongs the circulation time of the drug, and increases drug penetration. Nanocarriers are generally biodegradable in nature, and, thus, are risk-free. It also protects the drug from premature degradation, increasing its life span. Particle size and surface characteristics of NPs can be easily manipulated to achieve both passive and active drug targeting after parenteral administration (Mitchell et al. 2020).

17.2.3 Disadvantages of Drug Administration Employing Nanoscience

The advantages provided by the NPs are immense, yet some of the limitations need mention and may not be ignored. The large surface area of nanosized particles makes these particles highly sensitive to the biological environment. Similarly, some NPs, such as polymeric NPs, have limited drug-loading capacity, which is a serious disadvantage. Some forms of NPs may cause systemic toxicity, which is an important consideration for clinical use. The small size and increased surface area may also lead to the accumulation of particles, making the physical management of NPs difficult both in dry and liquid states (Mohanraj and Chen 2006). Nanoparticle synthesis may not be economical and may require sophisticated technology and skilled human resource for large-scale manufacturing.

17.3 Applications of Nanoparticles

17.3.1 Nanoparticles as Antibacterial Agents

At least 1% of the bacteria present in the ecosystem are responsible for causing illness in humans. What might appear small percentage includes a plethora of highly infectious organisms, including but not limited to *Escherichia coli*, *Pseudomonas aeruginosa*, *Klebsiella pneumoniae*, *Mycobacterium tuberculosis*, *Staphylococcus aureus*, and *Clostridioides difficile*. The frequent and prolonged use of commonly available antibiotics has led to antibiotic resistance in bacteria, making them less effective and creating a major public health problem. The pipeline for new drugs has been static for quite a while; therefore, there is a desperate need to find creative solutions to bacterial infections and combat antimicrobial resistance. According to the WHO's 2020 annual review of the clinical and preclinical antibacterial pipelines (World Health Organization 2021), five key criteria were highlighted: (a) Target

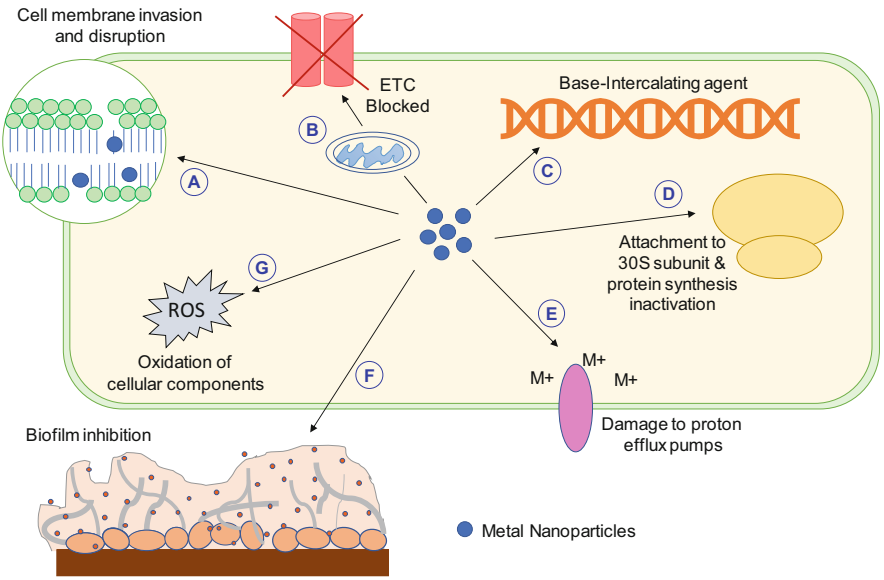

Fig. 17.3 Mechanisms of action and targets of metallic NPs in a bacterial cell. (**A**) Bacterial cell walls have an overall negative charge on them, attracting metal ions released from NPs to the membrane. The ions penetrate the membrane, creating pores and destabilizing its structure. (**B**) Mitochondrial toxicity by causing a loss in membrane potential and inhibiting ATPases thereby blocking the electron transport chain (ETC) and ATP generation. (**C**) The metal ions released from NPs enter the bacterial genome and intercalate between bases by attaching to their S or P groups leading to cytotoxic mutations. (**D**) Ions released from amassed NPs in the cytoplasm denature the ribosomal subunits and hinder protein synthesis. (**E**) NPs block the proton efflux pumps on bacterial membranes and thereby prevent them from extruding toxins. (**F**) NPs affect biofilm integrity by inhibiting EPS production and interrupting bacterial communication required for quorum sensing. (**G**) NPs can induce oxidative stress in the bacterial cell by generating reactive oxygen species, which oxidize glutathione, leading to suppression of the bacterial antioxidant defense system and allowing the metal ions to freely interact with cellular organs and disrupt their functions, leading to cell death

priority pathogens, (b) Overcome existing resistance, (c) Address a public health need, (d) Preserve effectiveness, and (e) Make accessible to all. Metal NPs with antibacterial activity meet all these criteria and have emerged as non-traditional but promising antibacterial agents. Different synthesis methods can produce NPs of varied shapes and dimensions, which shows strong and extended antimicrobial activity against a broad-spectrum of infectious bacteria (Correa et al. 2020). It has also been theorized that the ability of NPs to target multiple biomolecules in an organism can potentially bring the evolution of resistant bacteria to a standstill (Slavin et al. 2017). A diagrammatic representation of various mechanisms of action and targets of metal NPs in a bacterial cell is shown in Fig. 17.3. This chapter summarizes the latest understanding of the antimicrobial potential of NPs, wherein we have outlined the most recent and most cited papers that progressively endorse metallic NPs as the new antibiotic alternatives.

Silver (Ag) is the most sought-after metal for synthesizing NPs. In a study by Mohanta's group (2020), spherical silver NPs were synthesized in conjugation with fresh leaf extracts from three plants *Semecarpus anacardium* (SA), *Glochidion lanceolarium* (GL), and *Bridelia retusa* (BR). Successful synthesis was confirmed by observing a color change in the solution from the pale-yellow mixture of leaf extract to a deep brown color. Results from SEM micrographs determined their size range as 52–96 nm. The particles exhibited antibacterial and antibiofilm activity against three pathogenic bacteria: *E. coli*, *P. aeruginosa,* and *S. aureus*. SA-AgNPs showed the best antibacterial and antibiofilm with minimum inhibitory concentration (MIC) values. Antibacterial MICs are as follows, *E. coli*: 23.49 μg/mL, *P. aeruginosa*: 12.9 μg/mL, *S. aureus*: 33.72 μg/mL, and antibiofilm MICs are *E. coli*: 23.42 μg/mL, *P. aeruginosa*: 12.9 μg/mL, *S. aureus*: 33.77 μg/mL, respectively. Comparative analysis also indicated that GL-AgNPs were more active against gram-positive organisms (*S. aureus*), whereas SA-AgNP and BR-AgNPs had the most potent activity against gram-negative organisms (*P. aeruginosa* and *E. coli*) (Table 17.1). In a similar study, Ahmed's group (2020) involved green synthesis of silver NPs using the culture of silver-resistant *Bacillus safensis* TEN12 strain. UV-Vis spectroscopy was used to confirm the formation of AgNPs at an absorption peak at 426.18 nm, and FTIR analysis revealed that the AgNPs were stabilized by capping proteins and alcohols. The NPs were spherical, with sizes ranging between 20 and 45 nm, as confirmed by SEM and TEM. Disk diffusion and dilution assays revealed antibacterial activity against *S. aureus* with a zone of inhibition (ZOI) of 20.35 mm along with ~78% growth reduction and in *E. coli* ZOI was 19.69 mm and ~75% reduced growth. MTT assay with the NPs on the HepG2 cell line reported ~36% viability of cells. Both studies clearly showcase the strong potential of AgNPs as antibacterial therapeutic agents.

Rozilah's group (2020) reported the production of antibacterial polymer films made of sugar palm starch biopolymer composite films and AgNPs (0%, 2%, 3%, 4%). At higher AgNPs percentages, there was a noted increase in film elasticity and reduced molecular mobility of matrix, making the nanocomposite films more resistant to breaks, wear, and tear. FE-SEM was used to characterize the nanostructures of films, and the average size of AgNPs was 67.73 ± 6.39 nm. The nanocomposites with thickness ranging from 0.180 to 0.250 ± 0.05 mm were cut into circular disks and immersed in bacterial cultures to determine their activity against *S. aureus*, *E. coli,* and *S. cholerasuis*. Maximum inhibitory activity (ZOI ranging from 7 to 8 mm) was observed against gram-negative bacteria using bio-composite films with 3–4% AgNPs, which can further be explored to prepare films with food packaging applications. In retrospect, silver is a metal with attractive antibacterial potential, and therefore AgNPs must be pushed forward as commercial broad-spectrum antibacterial therapeutic agents. The anti-infective activity of AgNPs inspired the exploration of other metals for similar properties against infectious bacteria. Al-Musawi's group (2020) developed gold nanofibers by conjugating Honey/tripolyphosphate/chitosan (HTCs) fibers with *Capsicum annuum* (CA) and gold NPs. FE-SEM analysis revealed a size range of 351 ± 78 nm and a fibrous, dense, smooth, clear, and bead-free morphology. Disk diffusion assay confirmed

Table 17.1 Nanoparticles as antibacterial agents

Publication year	NPs and conjugates	Metal	Characterization	Size (nm)	Shape	Activities	Ref.
2020	Leaf extracts from *Semecarpus anacardium*, *Glochidion lanceolarium*, and *Bridelia retusa*	Silver	UV-vis, ATR-FTIR, DLS, SEM	52–96	Spherical	While GL-AgNPs were more active against gram-positive organisms, SA-AgNP and BR-AgNPs had the strongest activity against gram-negative organisms	Mohanta et al. (2020)
2020	Green synthesis using *Bacillus safensis* TEN12 strain culture	Silver	UV-vis, FTIR, XRD, SEM, TEM, EDXS	22–46	Spherical	Green NPs showed antibacterial (disk diffusion and MIC) activity against *E. coli* and *S. aureus*, and anticancer activity at 20 μg/mL AgNP concentration	Ahmed et al. (2020)
2020	The organic-inorganic hybrid of antibacterial sugar palm starch biopolymer composite films and silver NPs	Silver	FTIR, TGA, FE-SEM	67 ± 6.39	Spherical	ZOI for gram-negative bacteria in the range of 7–8 mm was observed with 3% and 4% of AgNPs	Rozilah et al. (2020)
2020	Honey/tripolyphosphate/chitosan (HTCs) nanofibers loaded with capsaicin derived from *Capsicum annuum* and loaded with gold NPs	Gold	FE-SEM	351 ± 78	Fibrous, dense, smooth, clear, and bead-free	The HTC-CA/AuNP were significantly effective against three gram-negative and one gram-positive organisms. Nanofibers also showed good wound-healing ability	Al-Musawi et al. (2020)

(continued)

Table 17.1 (continued)

Publication year	NPs and conjugates	Metal	Characterization	Size (nm)	Shape	Activities	Ref.
2020	Edible biopolymer (pullulan/carrageenan), D-limonene (DL), and copper sulfide NPs	Copper	FE-SEM, FTIR, XRD, WVP, WCA, MC	47.5 μm film thickness	Greenish intact films	Antibacterial activity against *E. coli* and a popular foodborne pathogen, *L. monocytogenes* was also observed	Roy and Rhim (2020)
2020	Citric acid-coated silver and iron oxide NPs	Silver and Iron	TEM, AFM, XRD	~10	Spherical, cubic, and spiral	Inhibited the growth of *E. coli* and *S. typhimurium* at a concentration of 100 μg/mL	Gabrielyan et al. (2020)
2020	Zinc NPs conjugated with pineapple peel waste and synthesized at different temperatures	Zinc	FTIR, XRD, FE-SEM, EDXS, TEM	Non-heated: 8–45 nm and heated 73–123 nm	Non-heated: spherical and rod-shaped. Heated: Flower rod shapes	ZOI ranging from 8–15 mm were noted on a *B. subtilis* lawn using the disk diffusion method. 3% non-heated zinc NPs showed the best antibacterial activity with ZOI of 15 mm	Basri et al. (2020)
2020	Extract of mushroom, *Fomes fomentarius*, with aqueous solutions of titanium isopropoxide and silver nitrate	Titanium and silver	XRD, DR-UV-S, FTIR, SEM, TEM	80–120	Irregular, rough surface, and aggregated	Disk diffusion using titanium NPs showed ZOI of 15 and 11 mm for *E. coli* and *S. aureus* lawns, respectively	Rehman et al. (2020)
2020	Rifampicin encapsulated in mesoporous silica NPs	Silica	QCM-D, TIRF, TGA, FTIR-ATR	~47	Spherical and mesoporous	A 2.5-fold reduction in colony-forming units (CFU) was observed. Calcined NPs tended to	Joyce et al. (2020)

						aggregate on lipid membranes leading to delay in drug delivery	
2020	Selenium NPs coated with recombinant spider silk protein eADF4 (κ16)	Selenium	Zeta potential, SEM, TEM, EDXS, ATR-FTIR, FSD	46	Spherical and monodispersed	Inhibited *E. coli* growth to 0.3×10^8 CFU/mL. The minimum bactericidal concentration observed was 8 ± 1 μg/mL	Huang et al. (2020)
2020	Leaf extracts of two medicinal plants, *Cassia fistula* and *Melia azedarach*, conjugated with zinc NPs	Zinc	XRD, FTIR, SEM, UV-vis, DLS	10–68	Spherical, clustered, rough surface	Cassia fistula zinc NPs showed better activity against *E. coli* (ZOI: 44 mm), and Meliaazedarach zinc NPs were more effective against *S. aureus* (ZOI: 38 mm)	Naseer et al. (2020)

AFM atomic force microscopy, *ATR-FTIR* attenuated total reflection-Fourier transform infrared spectra, *DLS* dynamic light scattering, *DR-UV-S* diffuse reflectance UV-visible spectroscopy, *EDS* electron diffraction spectroscopy, *EDXS* energy-dispersive X-ray spectroscopy, *FE-SEM* field-emission scanning electron microscopy, *FTIR* Fourier transform infrared spectroscopy, *FSD* Fourier self-deconvolution, *MC* moisture content, *QCM-D* quartz crystal microbalance with dissipation, *SEM* scanning electron microscopy, *TEM* transmission electron microscopy, *TIFR* total internal reflection fluorescence, *UV-vis* ultraviolet-visible spectroscopy, *WVP* water vapor permeability, *WCA* water contact angle, *XRD* X-ray diffraction

antibacterial activity against *P. multocida*: 34 mm (HTC-CA/AuNPs), *K. rhinoscleromatis*: 31.5 mm (HTC-CA/AuNPs), *S. pyogenes*: 30.5 mm (HTC-CA/AuNPs), *V. vulnificus*: 34 mm (HTC-CA/AuNPs). Although, HTC-CA and HTC-AuNPs showed better results for *P. multocida*, *K. rhinoscleromatis*. MTT assay for HTC-CA/AuNP showed 61% cell viability, over 20% greater than the other nanofibers. HTC-CA/AuNP also demonstrated superior wound healing abilities compared to HTC-CA and HTC-AuNPs dressings thereby indicating the multi-pronged potential of these nanofibers.

Roy's group (2020) developed an antibacterial biofilm from Edible biopolymer (pullulan/carrageenan), D-limonene (DL) and copper sulfide NPs (CuSNPs). The CuSNPs and DL fillers enhanced the UV-light shielding and mechanical properties of the film without altering the thermal stability and transparency. The greenish films showed a reduction of 7 log cycles for *E. coli* and about 2 log cycles for *L. monocytogenes*, a common pathogenic food microbe. In another study, Gabrielyan's group (2020) demonstrated citric acid-coated Ag and iron oxide NPs with antagonistic activity towards two strains of *E. coli* K12 (Wild type) and pARG25 (kanamycin-resistant) and *Salmonella typhimurium*. AgNPs effect was more pronounced on all the strains but iron oxide NPs also suppressed the bacterial growth rate of *E. coli* wild type, *E. coli* (kanamycin-resistant), and *S. typhimurium* by 1.3-, 2.5-, and 4-folds, respectively. A study on zinc NPs by Basri's group (2020) explored an exciting approach of conjugating zinc NPs with pineapple peel waste under temperature control and embedding zinc NPs in starch films to test for their antibacterial activity. Morphological experiments by SEM and TEM showed the non-heated (28 °C) zinc NPs as a mixture of spherical and rod-shaped (8–45 nm), whereas the heated (60 °C) zinc NPs were flower rod shapes (73–123 nm), and the zinc-starch nanocomposite films were 6 mm in diameter. The nanocomposite films prepared with non-heated zinc NPs showed higher efficacy than heated zinc NPs against *B. subtilis* at three NP concentrations 1%, 3%, and 5%. *B. subtilis* lawn indicated that films formed with 3% zinc non-heated and heated NPs showed the best antibacterial activity with ZOI of 15 and 12.33 mm, respectively. Therefore, this strategy could be further explored as a narrow-spectrum antibacterial agent. An intriguing study by Rehman's group (2020) illustrated the synthesis of titanium NPs in combination with intracellular extract of a wild mushroom, *Fomes fomentarius*. FE-SEM showed titanium NPs as aggregated, irregularly shaped with a rough surface in the size range of 80–120 nm. Antibacterial disk diffusion assay showed promising titanium NPs against *E. coli* (ZOI: 15 mm) and *S. aureus* (ZOI: 11 mm). Other recent studies using Silica, Selenium, and Zinc NPs with conjugates significantly indicate their antibacterial potential against *E. coli* and *S. aureus* (Joyce et al. 2020; Huang et al. 2020; Naseer et al. 2020). The NPs in these studies could be strong prospects of broad-spectrum antibacterial agents against the most commonly observed, virulent gram-positive and gram-negative microorganisms.

17.3.2 Nanoparticles as Antifungal Agents

Fungal pathogens are the most common cause of bloodstream infections in hospitalized patients (Pfaller et al. 2020). The fungal toxins cause severe and life-threatening infections in humans and animals, leading to hepato- and nephrotoxicity, pulmonary infections, immunosuppression, and cancer (Khatoon et al. 2015; Claeys et al. 2020). Severe fungal infections begin with fungal colonization followed by microbial colonies leading to complex multicellular biofilms, which are very hard to fight off with conventional antifungal agents (Paul et al. 2018; Guerra et al. 2020). The use of several antifungal agents for the treatment of fungal infections has been proposed, but most of them are not approved due to limited clinical data (Arastehfar et al. 2020; Wall and Lopez-Ribot 2020). The production and characterization of NPs synthesized using a variety of metallic/nonmetallic components, and variable sizes and shapes have diversified their applications in healthcare and the food sector (Shakibaie et al. 2015). NPs facilitate efficient, targeted delivery of active ingredients with slow-release and long-lasting effectiveness (Silva Viana et al. 2020). Several research groups have evaluated the use of metal NPs alone and as conjugates with antifungal drugs, algal extracts having antifungal properties (Guerra et al. 2020; Cleare et al. 2020; Sattary et al. 2020). Silver is the most commonly applied metal for antifungal assessment, owing to its broad antimicrobial spectrum and less toxicity in mammals (Guerra et al. 2020; Silva Viana et al. 2020). However, the use of other metals like gold, zinc, titanium, and selenium (Pariona et al. 2019; Osonga et al. 2020), and nonmetallic substances like silica and chitosan has also been described (Kalagatur et al. 2018). Discussed below are relevant studies from the past year as available on PubMed, which reported a high antifungal potential of NPs and conjugates (Table 17.2).

Guerra's group (2020) tested the effectiveness of AgNPs against pathogenic *Candida tropicalis* and nonpathogenic probiotic *Saccharomyces boulardii*. The rationale behind the study was to search nanomaterials with significant inhibition of the growth of pathogen microorganisms without eradicating other nonpathogenic species like *S. boulardii*. Synthesized AgNPs have a polygonal-like shape with an average size of 35 ± 15 nm having 1.2% weight of metallic silver stabilized with 18.8% weight of polyvinylpyrrolidone (PVP) in 80% weight of distilled water. The results revealed that 25 μg/mL AgNPs are sufficient to inhibit 90% of the *C. tropicalis* cell growth in comparison to 60% by Fluconazole at 35 μg/mL and 95% inhibition by Amp B at 5 μg/mL. The results indicate selective inhibition of pathogenic fungi by AgNPs as approximately 50% of the *S. boulardii* cell population remains viable in the presence of AgNPs, which can initiate further cell multiplication. Hosseini's group (2020) investigated the antifungal effect of zinc oxide (ZnO) NPs and Nystatin on inhibiting the growth of *C. albicans* isolates, causing vulvovaginal candidiasis (VVC). All isolates were susceptible to treatment at the lowest MIC value of ZnO-NPs (0.02 μg/mL) and Nystatin (0.6 μg/mL), respectively. The results indicate that both ZnO-NPs and Nystatin might be suitable inhibitors of *Candida* sp., with the highest sensitivity to ZnO at MIC 90, ≥0.5 μg/mL compared to the non-treated control samples. Therefore, ZnO can act as a potential

Table 17.2 Nanoparticles as antifungal agents

Publication year	NPs and conjugates	Metal	Target pathogen	Characterization	Size (nm)	Shape	Activities	Ref.
2020	Silver NPs with *Ligustrum lucidum* leaf extract	Silver	*Setosphaeria turcica* (Phytopathogen)	TEM, UV-Vis	4–42	Spherical	Antifungal activity against *S. turcica* with IC_{50} at a concentration of 170.20 μg/mL	Huang et al. (2020)
2020	Silver NPs	Silver	*Candida tropicalis*, *Saccharomyces boulardii*	TEM, UV-Vis	35 ± 15	Polygonal	Capable of inhibiting 90% cell growth in *C. tropicalis*, whereas ~50% population of probiotic yeast is still viable, demonstrating selective inhibition of pathogens	Guerra et al. (2020)
2020	Nitic oxide NPs	Nitric oxide	*Candida auris*	DLS	200–2000	Spherical	Significant ($p < 0.05$) growth inhibition of *C. auris* strains with a >70% reduction in biofilm formation at 10 mg/mL of NPs	Cleare et al. (2020)
2020	Mesoporous silica NPs encapsulated with lemongrass and clove oil	Silica	*Gaeumannomyces graminis*	FTIR, BET, TGA, UV-Vis	50–70	Spherical	Antifungal effects of the encapsulated oils increased threefold after encapsulation into NPs with a 70% disease control in vivo	Sattary et al. (2020)
2020	Zinc oxide NPs and Nystatin	Zinc	*Candida albicans*	UV-Vis	NA	Spherical	VVC *Candida* sp. showed the highest sensitivity to ZnO at MIC 90 ≥0.5 μg/mL compared to the non-treated control samples	Hosseini et al. (2020)
2020	Gold NPs	Gold	*Candida albicans*, *C. glabrata*, *C. tropicalis*, *C. krusei*	TEM, XRD	10–50	Rod-shaped	Gold nanorods led to a significant reduction in filament formation, growth inhibition, and prevention of biofilm formation following the incubation of conidia with NPs	Piktel et al. (2020)
2021	Gold NPs synthesized by green algae *Chlorella sorokiniana*	Gold	*Candida tropicalis*, *C. glabrata*, *C. albicans*	UV-Vis, DLS, XRD, FTIR, SEM, ICP-MS, TEM	5–40	Spherical	Significant antifungal activity against the *Candida* sp. was observed	Gürsoy and Öztürk (2021)

2020	Tungsten trioxide-doped Zinc oxide NPs	Tungsten	*Aspergillus niger*, *A. flavus*, *Penicillium notatum*	EDS, SEM, TEM, XRD	18–30	Spherical and rod	Superior antifungal activity as compared to the standard drug Fluconazole	Arshad et al. (2020)
2020	Chitosan-stabilized gold NPs and Carbon NPs	Gold, Carbon	*Fusarium oxysporum* DSM 62338, *F. oxysporum* DSM 62060	AFM, DLS, UV-Vis	Gold: 80 Carbon: 23	Spherical	A reduction in colony diameter of phytopathogenic fungal strains of *F. oxysporum* and *F. oxysporum* affecting tomato production was recorded	Lipşa et al. (2020)
2021	Zinc-based NPs	Zinc	*Fusarium oxysporum*, *Curvularia lunata, Macrophomina phaseolina*	FTIR, TEM, UV-Vis, XRD	8–210	Quasi-spherical to hexagonal	Maximum mycelial inhibitory activity was recorded in order: *F. oxysporum* > *C. lunata* > *M. phaseolina*	Kalia et al. (2021)
2020	Titanium dioxide NPs green synthesized and by sol-gel method	Titanium	*Ustilago tritic* (Wheat rust)	EDS, FTIR, SEM, XRD	15	Spherical	Green prepared titanium NPs were found to have the best antifungal activity against *U. tritici* wheat rust, especially NPs synthesized with the extract of *C. quinoa*	Irshad et al. (2020)
2020	Copper NPs	Copper	*Colletotrichum gloeosporioides* (tropical fruit pathogen)	DLS, TEM	100–300	Spherical	A 100% growth inhibition of *C. gloesporioides* at a concentration of 200 ppm copper was observed	Nguyen et al. (2020)
2021	Selenium NPs synthesized by *Bacillus megaterium* ATCC 55000	Selenium	*Rhizoctonia solani* RCMB 031001	DLS, TEM, UV-Vis, XRD	41	Spherical	Influential antifungal activity against *R. solani* in vitro as well as in vivo	Hashem et al. (2021)

(continued)

Table 17.2 (continued)

Publication year	NPs and conjugates	Metal	Target pathogen	Characterization	Size (nm)	Shape	Activities	Ref.
2021	Zinc oxide NPs	Zinc	*Alternaria alternata* CGJM 3078, *Alternaria alternata* CGJM 3006, and *Fusarium verticilliodes* CGJM 3823	BET, EDS, FTIR, UV-Vis, XRD, SEM, TEM, TGA	47–65	Spherical	Maximum inhibition was recorded at a concentration of 0.002–5 mg/mL with the largest zone of inhibition against *A. alternata* CGJM 3006 followed by *F. verticilliodes* CGJM 3823 and *A. alternata* CGJM 3078	Akpomie et al. (2021)
2021	Copper NPs	Copper	*Aspergillus niger*, *Fusarium oxysporum*, and *Alternaria alternata*	UV-Vis, FTIR, NTA, TEM, XRD, Zeta potential	5–12	Spherical	Significant antifungal effect against the target pathogen is reported	Shende et al. (2021)

AFM atomic force microscopy, *BET* Brunauer-Emmett-Teller, *DLS* dynamic light scattering, *EDS* energy-dispersive X-ray spectrometry, *FTIR* Fourier transform infrared spectrometry, *ICP-MS* inductively coupled plasma mass spectrometer, *NA* not applicable, *NTA* NPs tracking and analysis system, *SEM* scanning electron microscopy, *TEM* transmission electron microscopy, TGA thermo gravimetric analysis, *UV-Vis* ultraviolet-visible spectroscopy, *XRD* X-ray diffraction

agent for the control, prevention, and treatment of VVC. Similar observations against Amp B-resistant *C. albicans* are recorded using gold, silver, and selenium NPs (Lotfali et al. 2021). Piktel's group (2020) demonstrated a significant reduction in filament formation following the incubation of conidia with average survival rates of 16.50 ± 11.12%, 10.8 ± 13.25%, 1.67 ± 0.19%, and 0.9 ± 0.51% for the tested *C. albicans*, *C. glabrata*, *C. tropicalis,* and *C. krusei* isolates at a dose of 1 ng/mL. No hemolytic activity was recorded at fungicidal doses, along with a reduction in biofilm formation at relatively low doses of 0.5–5 ng/mL. Cleare's group (2020) also demonstrated significant growth inhibition of *Candida auris* strains and a >70% decrease in biofilm viability after treatment with 10 mg/mL of nitric oxide NPs. Green synthesized gold NPs synthesized using algae *Chlorella sorokiniana* displayed prominent activity against *Candida tropicalis*, *C. glabrata*, and *C. albicans* (Gürsoy and Öztürk 2021). The effectiveness of metallic NPs against *Aspergillus* sp. is also widely explored. Although lower than the conventional fluconazole antifungal drug, tungsten trioxide-doped zinc oxide NPs are found effective against *Aspergillus* sp. (*A. niger* and *A. flavus*) and *Penicillium notatum* (Arshad et al. 2020). Further, improvements with such rarely used metal NPs can be made by optimizing the metal concentration and reaction conditions.

Apart from the human pathogenic fungi, the use of antifungal NPs has overcome the persistent limitations of using conventional chemical fungicides in the management of plant diseases. Studies have reported the antifungal activity of metal NPs against a soil-borne plant pathogen, *Fusarium oxysporum*. A reduction in colony diameter of phytopathogenic fungal strains of *Fusarium* (*F. oxysporum* DSM 62338 and *F. oxysporum* DSM 62060) that affect tomato production was recorded when treated with chitosan-stabilized gold (AuNPs) and Carbon (CNPs) (Lipșa et al. 2020). A mycelial growth inhibition rate of 100% was achieved in the case of *F. oxysporum* DSM 62060 using 5 mL of three different concentrations of NPs (AuNP25, AuNP50, AuNP75). However, maximum growth inhibition of 54.1% was observed in the case of *F. oxysporum* DSM 62338. CNPs resulted in maximum inhibition of 42.4% and 36.5% for *F. oxysporum* DSM 62338 and *F. oxysporum* DSM 62060. Another study by Kalia's group (2021) reported extensive leakage of the cytoplasmic material from the hyphal tissue along with the swelling of the hyphae cells in the tested fungal species (*Fusarium oxysporum* > *Curvularia lunata* > *Macrophomina phaseolina*) at a 40 mg/L concentration of zinc oxide NPs. Wheat rust caused by *Ustilago tritici* is responsible for global losses in wheat production and harvesting. Irshad's group (2020) has reported a high antifungal potential of green synthesized titanium dioxide-based NPs, especially those produced using *C. quinoa* extract. Similarly, phytopathogenic *Setosphaeria turcica* is responsible for severe foliar disease in maize crops. Spherical AgNPs with an average size of 13 nm, synthesized with *Ligustrum lucidum* leaf extract, effectively against *S. turcica* with IC_{50} of 170.20 μg/mL (Huang et al. 2020). Sattery's group (2020) reported antifungal effects of the mesoporous silica NPs encapsulated with lemongrass and clove oil increased threefold after encapsulation into NPs with a 70% disease control confirmed by in vivo studies. One of the most delicious tropical fruit, mango, suffers severe damage due to anthracnose produced by

phytopathogenic *Colletotrichum gloeosporioides* (Kamle and Kumar 2016). Anthracnose is responsible for huge (sometimes up to 100%) postharvest loss for mangoes produced under wet or humid conditions. A promising dose-dependent antifungal activity of copper NPs in the size range of 100–300 nm has been reported against *C. gloeosporioides* with 100% growth inhibition at 200 ppm copper (Nguyen et al. 2020). Hashem's group (2021) reported antifungal activity of selenium NPs against *Rhizoctonia solani* RCMB 031001 both in vitro and in vivo with minimum inhibition and minimum fungicidal concentrations of 0.0625 and 1 mM, respectively. A decrease in the severity of root rot disease was noted after treatment. Another report (Akpomie et al. 2021) on plant pathogenic fungi describes a maximum inhibition of *Alternaria* sp. and *F. oxysporum* after treatment with zinc NPs. The largest zone (25.09–36.28 mm) against *A. alternata* CGJM 3006 was observed at a concentration of 0.002–5 mg/mL, followed by *F. verticilliodes* CGJM 3823 (23.77–34.77 mm) and *A. alternata* CGJM 3078 (22.73–30.63 mm) in comparison to a positive control (5% bleach). Lastly, copper NPs have shown promising activity against *A. niger*, *F. oxysporum*, and *A. alternata* (Shende et al. 2021).

17.3.3 Nanoparticles as Antiviral Agents

Viruses are the disease-causing agent and have been the causative agent of various diseases in humans. They have a global presence and are responsible for pandemics and epidemics in the past. Viral infections have high morbidity and mortality rate as more than half a million (0.69 million) people died from AIDS-related illnesses in 2019 (Mahy et al. 2019). Respiratory viral infections are easily transmissible and result in a high death rate. Since the exposure of Corona virus disease 2019 (COVID-19), 50 million people were affected, and 3.15 million deaths were observed until April 2021, making it the highest pandemic of the century (Riffe and Acosta 2021). They also cause severe infections, as seen in the case of the Zika virus that results in encephalopathy and meningitis (Nunes et al. 2016). This also affects socioeconomic ratios and impacts the quality of life, as we have seen in the recent pandemic of COVID-19. Considering how prevalent these viral infections are, there is a smaller number of antiviral drugs available. The available vaccines need to be upgraded as the virus mutates rapidly, leading to a new strain, making the available vaccine less effective. Although the search and development of new antiviral are difficult but new and promising therapies have been suggested. NPs have very compelling properties that include optimal size, shape, immuno-compatibility, biodegradability, slow release in bloodstream, and importantly can cross blood-air as well as the blood–brain barrier thus can be precise for a target. NPs alone or in conjugation with antiviral drugs seem to be potential antiviral therapy candidates (Jiao et al. 2018; Szunerits et al. 2015; Gurunathan et al. 2018). The snapshot of antiviral mechanisms of NPs is presented in Fig. 17.4. Thus, to explore the role of the potential impact of NPs in antiviral therapy, we have discussed past 1-year studies retrieved from PubMed using keywords as antiviral and nanoparticles in the advance search option (Table 17.3).

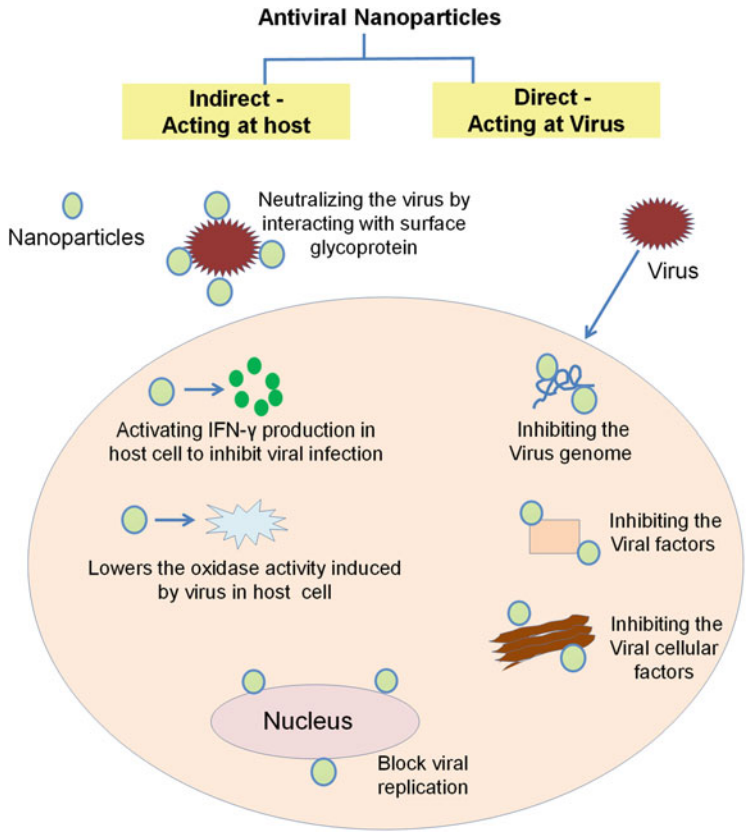

Fig. 17.4 Pictorial representation of NPs as antiviral agents

The study done by Bharti's group (2021) explored the potential of colloidal and immobilized glass silver NPs against water-borne bacteriophages. The particles were synthesized using a chemical reduction approach and immobilized by post-immobilized method on a glass substrate having amines as a functional group. SEM and TEM platforms characterized NPs. Colloidal silver NPs inactivated the T4 bacteriophage and MS2 at the concentration of 60 μg/mL, making the drinking water free from these viruses. As the COVID pandemic is going on, there is an urgent need for a vaccine. So, many NPs emerged as potential candidates against SARS-CoV2. In a study done by Wang's group (2021), cell membrane-based NPs were formed by the classical extrusion method, in which HEK-293 T-hACE2 cells were used for experimentation. These NPs exhibit affinity towards ACE2 receptors to attach to S1 of spike protein,-making the virus less available to HK-2 cells and reducing the infection. The TEM analysis revealed a diameter of size 100 nm. The conjugated NPs efficiently reduced the adherence of severe acute respiratory syndrome corona virus 2 (SARS-CoV2) and its mutant D614G-S1 (which is prevalent globally) to HK-2 cells. IC_{50} to neutralize the SARS-CoV2 pseudovirions is 431.2

Table 17.3 Nanoparticles as antiviral agents

Publication year	NPs and conjugates	Metal	Target pathogen	Characterization	Size (nm)	Shape	Activities	Ref.
2021	Colloidal Silver NPs	Silver	MS2, andT4 bacteriophage	SEM, TEM	1–10	Spherical	At the dose of 60 μg/mL completely inactivate MS2 and T4 bacteriophage within 30 and 50 min with an initial concentration of 10^3 PFU/mL	Bharti et al. (2021)
2021	Cell membrane-based NPs	NA	SARS-CoV2, D614G-S1, pseudovirions	TEM, DLS	100	Spherical	Effectively neutralized the virus with an IC_{50} 431.2 μg/mL. Also inhibited the apoptosis induced by translocation of S1 into the cytoplasm of the virus	Wang et al. (2021)
2020	Nanodecoy (cellular membrane nanovesicles)	NA	SARS-CoV2	TEM	100	Round	Neutralize inflammatory cytokines, including IL-6 and GM-CSF. In vivo suppress acute pneumonia in mice model	Rao et al. (2020)
2020	Silver NPs	Silver	SARS-CoV2	TEM	2–15	Spherical	AgNPs inhibits the SARS-CoV2 in veroE6 cell/TMPRS22, at a concentration of 2 ppm	Jeremiah et al. (2020)
2020	Ivermectin-loaded PLGA-*b*-PEG-MAL-NPs	NA	SARS-CoV2	TEM	70–80	Spherical	Inhibit the expression of spike protein and ACE2 at the transcription level	Surnar et al. (2020)
2021	*Linga chenduram* NPs	Mercury and sulfur	Hepatitis C virus	SEM, TEM, FTIR, XRD, EDAX	9–18	Spherical	Inhibit the viral activity in a dose-dependent manner	Al-Ansari et al. (2021)
2021	Poly (lactic-co-glycolic acid) curcumin NPs	NA	Zika Virus	FTIR, SEM, DLS, DSC	210 ± 40	Polygonal	PLGA-curcumin inhibits ZIKA virus growth and reduces the viral RNA synthesis and protein expression	Pacho et al. (2021)

2020	Monoolein based NPs	NA	HIV	TEM	155 ± 7	Spherical	Monoolein-indinavir suppresses the growth of HIV virions	Bianchin et al. (2021)
2020	Silver NPs	Silver	H1N1	TEM	20–25	Spherical	AgNPs lower the oxidase activity and increase the life expectancy of mice	Kiseleva et al. (2020)
2021	Nano-Mn	Manganese	MHV-A59 (Murine coronavirus)	TEM, DLS	20–30	Spherical	Nano-Mn activates the IFN-γ production and also suppresses the virus infection in C57/BL-6 mice.	Sun et al. (2021)

DLS dynamic light scattering, *DSC* differential scanning calorimetry, *EDAX* energy-dispersive X-ray analysis, *FTIR* Fourier transform infrared spectroscopy, *SEM* scanning electron microscope, *TEM* transmission electron microscope, *XRD* X-ray diffraction

ng/mg. It is nontoxic, both in vitro and in vivo, making it a potential candidate against the virus. A similar study against SARS-CoV2 by Rao's group (2020) has taken membrane vesicle nanodecoy with 100 nm in size analyzed by TEM. They have shown that it binds and neutralizes inflammatory cytokines, including interleukin 6 (IL-6) and granulocyte-macrophage colony-stimulating factor (GM-CSF). In vivo study also showed that it suppresses pneumonia in mice models. In an interesting study done by Jeremiah's group (2020), to determine the size and concentration at which silver NPs inhibit the SARS-CoV2. They have taken different sizes and concentrations and found that at around 10 nm, a concentration ranging from 1 to 10 ppm showed an inhibitory effect. The concentration above 20 ppm causes cytotoxicity in veroE6 cells/TMPRS22, and they also showed that AgNPs inhibit the viral entry by destroying the integrity of the virus, confirmed by luciferase-based assay. Surnar's group (2020) using ivermectin drug loaded with poly(lactide-*co*-glycolide)-*b*-poly(ethylene glycol)-maleimide (PLGA-*b*-PEG-Mal) polymer and tagged with Fc immunoglobulin fragment. Ivermectin is a clinically antiviral-approved drug, but its single dose is toxic to the body, and fast clearance results in the noneffectiveness of the drug. So, the NPs are loaded with medicine cause it is slowly released into the bloodstream. Further attachment to Fc helps in crossing the gut epithelial barrier to reach the bloodstream. It has been shown in the study that free ivermectin is less effective in inhibiting or reducing the expression of pseudo-SARS-CoV2 as well as HEK293T expressing spike protein than ivermectin NPs. There are other studies also which proposed that Silver NPs are a potential candidate for inhibiting SARS-CoV2 shown by homology modeling and other bioinformatics studies (Pilaquinga et al. 2021; Varahachalam et al. 2021). Plants extract with known antiviral properties has been taken in nano form against Hepatitis C virus, as seen in a study by Al-Ansari's group (2021). Traditional medicine formed from the herbal mineral Linga chenduram was used. It consists of mercury and sulfur elements in large amounts, but other metals like silver, iron, and molybdenum were also present in trace amounts shown by EDAX analysis. The particles are in the range of 9.71–18.40 nm, having spherical, but other shapes like triagonal, cubic, and hexagonal also exist. The inhibitory effect was seen on Huh-7 hepatoma cell line, showing a strong impact in a dose-dependent manner. It is nontoxic to the cell line and in vivo in the male albino rat. In a study against the ZIKA virus, curcumin is used, which has antiviral antibacterial activity. The NPs are made using Poly-lactic-co-glycolic acid (PLGA) as a polymer matrix. The size of the NP is 210 ± 40 nm, as observed from SEM, whereas DLS shows 780 nm size. This difference arises due to the aggregation of NPs in DLS as performed at 25 °C. In an in vitro study, in Vero cells, the E_{50} value was 3.7 ± 0.05 mm. The antiviral activity of PLGA-curcumin is more than free curcumin. Also, the synthesis of virus protein in Vero cells reduces as there has been a reduction of 68% in E-protein synthesis when incubating with PLGA-curcumin compared to only 20% reduction seen with free curcumin (Pacho et al. 2021). In a fascinating study done by Bianchin's group (2021), they made children-friendly drugs for HIV using monoolein-based NPs containing indinavir drug, a particle size of 155 ± 7 nm. The monoolein successfully masked the bitter taste of the known anti-HIV drug indinavir, making it suitable for children to eat. Another study against

the influenza virus done by Kiseleval's group (2020) using silver NPs reported that it lowers the oxidase activity, prevents the lesion, and increases the life expectancy of female CBA mice. The characterization is done by TEM with a mean average size of 20–25 nm.

17.3.4 Nanoparticles as Anti-leishmanial Agents

Leishmaniasis is a widespread neglected tropical disease caused by protozoan parasites belonging to the genus *Leishmania*. Clinically, the disease is classified into three primary forms, cutaneous, mucocutaneous, and visceral leishmaniasis. Among them, visceral leishmaniasis is the fatal one and annually, 20,000–30,000 deaths occur due to this disease. Treatment regimens rely upon a few numbers of drugs such as pentavalent antimonials, Amp B, Miltefosine, and Paromomycin (Singh et al. 2016; Altamura et al. 2020). With increasing drug resistance and toxicities against these drugs, it is the need of the hour to improve the drug delivery approach to fight against leishmaniasis. In the following section, we have tried to discuss the last 1-year research publications retrieved from PubMed, which elucidate the role of NPs in anti-leishmanial therapy (Table 17.4).

Saqib's group (2020) assessed the anti-leishmanial activity of polycaprolactone (NPs) containing Amp B against two strains of the parasite (*L. donovani* and *L. tropica* KWH23). NPs formed were spherical with an average size of 183 nm and encapsulation efficiency of ~86% analyzed by UV-visible spectrophotometer. Macrophages cell line (J774) was infected with *L. donovani* and *L. tropica* KWH23 parasites, and anti-leishmanial activities of NPs, Amp B, and Ambisome were evaluated in a dose-dependent manner. As reported, inhibitory concentration (IC_{50}) of NPs, Amp B, and Ambisome against *L. donovani* are 0.23, 0.21, and 0.28, respectively, and against *L. tropica* KWH23 these values are 0.03, 0.19, and 0.25 μg/mL, respectively. IC_{50} of NPs against *L. tropica* KWH23 was significantly lower as compared to the standard drugs. Thus, this formulation can provide a novel option for treating cutaneous infections caused by the *L. tropica* parasite. In another study, Almayouf's group (2020) determined the effect of silver NPs against cutaneous infection of leishmaniasis in female Balb/c mice. Silver NPs containing Fig and Olive extracts were biosynthesized, and TEM studies confirmed the spherical shape of NPs, along with size ranging from 50 to 100 nm. Infection in Balb/c mice was developed by giving a subcutaneous injection of *L. tropica* parasites above the tail area. After the completion of 3 weeks, the mice group which were pretreated with NPs reported significantly reduced skin lesions as compared to the untreated group. Pretreatment with NPs also reduced oxidative stress and increased antioxidant enzyme activities in *L. major* infected Balb/c mice. NPs pretreated mice group also showed a marked decrease in the mRNAs expression levels of interleukin (IL)-1β and tumor necrosis factor (TNF)-α. In another study, Awad's group (2021) synthesized silver NPs using *Commiphora molmol* (myrrh) and performed in vitro and in vivo assays against *L. major*. Dose-dependent reduction in the growth of *L. tropica* promastigotes was observed during in vitro studies and in vivo studies in

Table 17.4 Nanoparticles as anti-leishmanial agents

Publication year	NPs and conjugates	Metal	Characterization	Size (nm)	Shape	Activities	Ref.
2020	Polycaprolactone NPs containing Amp B	NA	SEM	183	Spherical	Inhibited the growth of both *Leishmania tropica* and *Leishmania donovani* amastigotes with an IC_{50} value of 0.03 and 0.023 μg/mL, respectively	Saqib et al. (2020)
2020	Silver NPs containing Fig and Olive extracts	Silver	TEM	50–100	Spherical or polygonal	Effective in reducing lesions in mice infected with *Leishmania major* and also enhanced the activity of antioxidant enzymes	Almayouf et al. (2020)
2021	Silver NPs containing *Commiphora molmol* (myrrh)	Silver	TEM, EDS	49	Spherical	During in vitro studies, dose-dependent (10–150 μL/100 μL) inhibition of *Leishmania major* promastigote was observed and in vivo studies report the healing of skin lesions in mice model	Awad et al. (2021)
2021	Cadmium oxide and chitosan NPs	Cadmium	SEM, TEM, EDS	18–40	Spherical	Reduced the growth of *Leishmania major* promastigote with an IC_{50} value of 0.6 μg/mL and also induced apoptosis-mediated cell death	Bahraminegad et al. (2021)
2020	Chitosan NPs containing Amp B	NA	SEM, TEM	69 ± 8	Spherical	Amp B-loaded chitosan NPs were more effective in reducing lesions and parasite	Riezk et al. (2020)

						load in mice model of CL as compared to AmBisome®.	
2020	Titanium dioxide NPs doped with Zinc and hypericin	TiO_2	SEM, TEM, EDS	~20	Spherical	Inhibited the growth of *Leishmania amazonensis* with an IC_{50} value of 17.5 μg/mL and reduced the parasite load by 43–58% in the BALB/c mice model of CL	Sepulveda et al. (2020)
2020	Silver NPs containing xylan	Silver	SEM, AFM, EDS	~102	Spherical	Inhibited the growth of *Leishmania amazonensis* promastigote with an IC_{50} value of 25 μg/mL	Silva Viana et al. (2020)
2020	Silver NPs containing extract of *Mentha arvensis* and *Mentha longifolia*	Silver	SEM, AFM, EDS	20–100	Spherical	Significantly reduced the growth of *Leishmania tropica* promastigote with an in vitro IC_{50} activity of 10–13 μg/mL	Javed et al. (2020a, b)
2020	Biogenic gold-silver bimetallic NPs	Gold and Silver	TEM, EDS	10–12	Spherical	Inhibited the growth of *Leishmania donovani* promastigote as well as amastigote with an IC_{50} value of 0.03–0.035 μg/mL	Alti et al. (2020)
2020	Gold NPs containing Amp B	Gold	DLS, FTIR, TEM	~48	Spherical	Significantly reduced the growth of *Leishmania donovani* promastigote with an IC_{50} value ~20 nM and also activated immunostimulatory Th1 (IL-12 and interferon-γ) response	Kumar et al. (2019)

(continued)

Table 17.4 (continued)

Publication year	NPs and conjugates	Metal	Characterization	Size (nm)	Shape	Activities	Ref.
2020	Guar gum NPscontaining Amp B and piperine	NA	DLS	<200	Spherical	During In vitro assay, the growth of *Leishmania donovani* promastigote was inhibited with an IC_{50} value of 24 ng/mL and in vivo studies in a golden hamster model of VL displayed ~90 parasite inhibition	Ray et al. (2020)
2020	2-Hydroxypropyl-β-cyclodextrin (HPCD) modified solid lipid NPs with Amp B and paromomycin	NA	SEM, TEM	141 ± 3.2	Spherical	Inhibited the growth of intracellular *L. donovani* amastigotes with an IC_{50} value of 0.013 μg/mL and also significantly reduced the parasite load by 70–90% in BALB/c mice model of VL	Parvez et al. (2020a)
2020	Chitosan solid lipid NPs containing Amp B and paromomycin	NA	SEM, TEM	373 ± 1.4	Spherical	Ex vivo anti-leishmanial activity on intracellular amastigotes of *L. donovani* was reported to be 0.018 μg/mL; which is significantly lower as compared to Amp B alone	Parvez et al. (2020b)

AFM atomic force microscopy, *DLS* dynamic light scattering, *EDS* electron diffraction spectroscopy, *EDS* energy-dispersive X-ray spectroscopy, *FTIR* Fourier transform infrared spectroscopy, *NA* not applicable, *SEM* scanning electron microscopy, *TEM* Transmission Electron Microscopy

BALB/c mice also reported complete healing of the skin lesions within 3 weeks of infection. In both studies mentioned above, lesion healing was significantly better as compared to the standard drug pentostam. Other recent studies also signify the protective efficacy of NPs against cutaneous infection caused by the *Leishmania* parasite (Bahraminegad et al. 2021; Riezk et al. 2020; Sepulveda et al. 2020; Silva Viana et al. 2020). In an interesting study, Javed's group (2020a) explored the role of non-oxidative biocompatible silver NPs synthesized from an aqueous extract of *Mentha arvensis* against *L. tropica*. The average size of NPs was 20–100 nm, and they were structurally anisotropic, confirmed by SEM and AFM studies. Biocompatible NPs were highly effective against *L. tropica* promastigotes as 10 μg/mL dose of NPs killed ~50% of the parasite. In a similar study by the same group (Javed et al. 2020b), silver NPs were phyto-synthesized from an aqueous extract of *Mentha longifolia*. They reported dose-dependent killing of *L. tropica* parasites, with 10 μg/mL dose of NPs killing ~67% of the parasite. Both silver, as mentioned earlier NPs were also effective in killing various plant bacterial pathogens (Javed et al. 2020a, b).

As the drug resistance cases against the current treatment regimen for visceral leishmaniasis are on the rise, Alti's group (2020) synthesized biogenic bimetallic NPs using herbal leaf extracts to evaluate the anti-leishmanial effect against promastigote and amastigote forms of *L. donovani*. TEM and EDX studies confirmed that NPs formed were well separated, spherical, and had an average size of 10–12 nm. As reported, IC_{50} of bimetallic NPs against promastigote was significantly lower (0.035 μg/mL) than the standard drug miltefosine (10 μg/mL). Bimetallic NPs were also successful in reducing the amastigote form of the parasite by 30–45% in *L. donovani* infected THP-1 cell line. Mechanistic studies revealed that parasite cell death occurred due to reactive oxygen species-induced apoptosis.

Similarly, Kumar's group (2019) also reported improved anti-leishmanial efficacy (~5 folds) of gold NPs conjugated with Amp B compared to Amp B alone during ex vivo studies. The above studies suggest that the metallic NPs-based drug delivery approach can be explored as an alternative option to the available standard drugs. In an attempt to increase the bioavailability of Amp B, Ray's group (2020) developed enteric-coated guar gum NPs containing natural bioenhancer (piperine) and Amp B suitable for oral administration. These NPs displayed controlled drug release and also protected the drug from the acidic pH of the stomach. In vitro studies of these NPs against promastigotes and amastigotes of *L. donovani* parasites exhibited two to threefolds higher IC_{50} than Amp B drug alone. Golden hamster animal model infected with *L. donovani* also showed significant anti-leishmanial activity with ~90% parasite clearance along with enhanced drug bioavailability confirmed by pharmacokinetics and biodistribution studies. In another study, Parvez's group (2020a) reported the use of 2-hydroxypropyl-β-cyclodextrin (HPCD)-based solid lipid NPs composed of Amp B and paromomycin as an oral drug delivery approach. NPs were spherical with an average size of 141 ± 3.2 nm, confirmed by SEM and TEM studies. The safety and biocompatibility of formulated NPs were confirmed by cytotoxicity studies performed in the J774A.1 macrophage cell line and Swiss albino mice model. Ex vivo studies reported the inhibition of

growth of *L. donovani* amastigotes with an IC_{50} value of 0.013 μg/mL, and in vivo experiments performed in BALB/c mice infected with *L. donovani* also showed a 70–90% decrease in parasite burden. In a similar study by the same group (Parvez et al. 2020b), the use of chitosan-based NPs containing Amp B and paromomycin drugs proved effective in inhibiting the growth of the *L. donovani* parasite. Thus, the above studies suggest that NPs-based oral drug delivery approach is the way forward to fight against leishmaniasis.

17.4 Conclusion and Future Perspectives

It is evident from the above context that the synergistic effect of nanotechnology with nanoscience has revolutionized the path of therapeutics approaches. With the excellent efficacy of NPs as antibacterial, antifungal, antiviral, and anti-leishmanial candidates, it is the future ray of hope in overcoming drug resistance and enhancing the killing efficacy of the drug. The use of metallic, liposomal, solid lipid NPs and polymeric micelles aided in on-point drug delivery, treatment shortening controlled drug release, and reduced considerable toxicity. The major action mechanisms employing NPs are enhancing oxidative/nitrosative production in parasites and bacteria, inhibiting biofilm formation in fungi and bacteria, and remodeling viral capsid proteins to disrupt its function and halt replication machinery of the virus. However, NPs are mostly restricted to the study and do not enter clinical trials owing to extensive cost, complicated synthesis mechanism, and low drug loading capacity. Despite these limitations, NPs carry significant potential pertaining to drug delivery approaches. Developing improved preclinical animal models along with a well-versed biological concept can improve the NPs-mediated drug delivery system. Eventually, alliance with theoretical and experimental researches across academia, pharmaceutical industry, and medicine will assist in taking forward these discoveries from research laboratories to the standard population. Therefore, there is an imperative urge to overdue these downfalls and explored realistic applications of NPs for next-generation drug delivery platforms.

References

Abbasi E, Aval SF, Akbarzadeh A, Milani M, Nasrabadi HT, Joo SW, Hanifehpour Y, Nejati-Koshki K, Pashaei-Asl R (2014) Dendrimers: synthesis, applications, and properties. Nanoscale Res Lett 9:1–10

Ahmad MZ, Rizwanullah M, Ahmad J, Alasmary MY, Akhter MH, Abdel-Wahab BA, Warsi MH, Haque A (2021) Progress in nanomedicine-based drug delivery in designing of chitosan nanoparticles for cancer therapy. Int J Polym Mater Polym Biomater 71:1–22

Ahmed T, Shahid M, Noman M, Niazi MBK, Zubair M, Almatroudi A, Khurshid M, Tariq F, Mumtaz R, Li B (2020) Bioprospecting a native silver-resistant Bacillus safensis strain for green synthesis and subsequent antibacterial and anticancer activities of silver nanoparticles. J Adv Res 24:475–483

Akpomie KG, Ghosh S, Gryzenhout M, Conradie J (2021) One-pot synthesis of zinc oxide nanoparticles via chemical precipitation for bromophenol blue adsorption and the antifungal activity against filamentous fungi. Sci Rep 11:1–17

Al-Ansari MM, Singh AR, Al-Khattaf FS, Michael JJ (2021) Nano-formulation of herbo-mineral alternative medicine from linga chenduram and evaluation of antiviral efficacy. Saudi J Biol Sci 28:1596–1606

Almayouf MA, El-Khadragy M, Awad MA, Alolayan EM (2020) The effects of silver nanoparticles biosynthesized using fig and olive extracts on cutaneous leishmaniasis-induced inflammation in female balb/c mice. Biosci Rep 40. https://doi.org/10.1042/BSR20202672

Al-Musawi S, Albukhaty S, Al-Karagoly H, Sulaiman GM, Alwahibi MS, Dewir YH, Soliman DA, Rizwana H (2020) Antibacterial activity of honey/chitosan nanofibers loaded with capsaicin and gold nanoparticles for wound dressing. Molecules 25:4770

Altamura F, Rajesh R, Catta-Preta CMC, Moretti NS, Cestari I (2020) The current drug discovery landscape for trypanosomiasis and leishmaniasis: challenges and strategies to identify drug targets. Drug Dev Res 83:1–28

Alti D, Veeramohan Rao M, Rao DN, Maurya R, Kalangi SK (2020) Gold–silver bimetallic nanoparticles reduced with herbal leaf extracts induce ROS-mediated death in both promastigote and amastigote stages of Leishmania donovani. ACS Omega 5:16238–16245

Arastehfar A, Gabaldón T, Garcia-Rubio R, Jenks JD, Hoenigl M, Salzer HJ, Ilkit M, Lass-Flörl C, Perlin DS (2020) Drug-resistant fungi: an emerging challenge threatening our limited antifungal armamentarium. Antibiotics 9:877

Arshad M, Ehtisham-ul-Haque S, Bilal M, Ahmad N, Ahmad A, Abbas M, Nisar J, Khan M, Nazir A, Ghaffar A (2020) Synthesis and characterization of Zn doped WO3 nanoparticles: photocatalytic, antifungal and antibacterial activities evaluation. Mater Res Express 7:015407

Awad MA, Al Olayan EM, Siddiqui MI, Merghani NM, Alsaif SSA-L, Aloufi AS (2021) Antileishmanial effect of silver nanoparticles: green synthesis, characterization, in vivo and in vitro assessment. Biomed Pharmacother 137:111294

Bagchi T, Chauhan S (2018) Nanotechnology-based approaches for combating tuberculosis: a review. Curr Nanomater 3:130–139

Bahraminegad S, Pardakhty A, Sharifi I, Ranjbar M (2021) The assessment of apoptosis, toxicity effects and anti-leishmanial study of Chitosan/CdO core-shell nanoparticles, eco-friendly synthesis and evaluation. Arab J Chem 14:103085

Basha SK, Dhandayuthabani R, Muzammil MS, Kumari VS (2020) Solid lipid nanoparticles for oral drug delivery. Mater Today Proc 36:313–324

Bharti S, Mukherji S, Mukherji S (2021) Antiviral application of colloidal and immobilized silver nanoparticles. Nanotechnology 32:205102

Bianchin MD, Prebianca G, Immich MF, Teixeira ML, Colombo M, Koester LS, Araújo BVD, Poletto F, Külkamp-Guerreiro ICJDD, Pharmacy I (2021) Monoolein-based nanoparticles containing indinavir: a taste-masked drug delivery system. Drug Dev Ind Pharm 47:83–91

Cartaxo ALP (2016) Nanoparticles types and properties—understanding these promising devices in the biomedical area

Chen L, Liang J (2020) An overview of functional nanoparticles as novel emerging antiviral therapeutic agents. Mater Sci Eng C 112:110924

Claeys L, Romano C, De Ruyck K, Wilson H, Fervers B, Korenjak M, Zavadil J, Gunter MJ, De Saeger S, De Boevre M (2020) Mycotoxin exposure and human cancer risk: a systematic review of epidemiological studies. Comp Rev Food Sci Food Saf 19:1449–1464

Cleare LG, Li KL, Abuzeid WM, Nacharaju P, Friedman JM, Nosanchuk JD (2020) NO Candida auris: nitric oxide in nanotherapeutics to combat emerging fungal pathogen Candida auris. J Fungi 6:85

Correa MG, MartÃnez FB, Vidal CPO, Streitt C, Escrig J, de Dicastillo CL (2020) Antimicrobial metal-based nanoparticles: a review on their synthesis, types and antimicrobial action. Beilstein J Nanotechnol 11:1450–1469

Farias IAP, Santos CCLD, Sampaio FBC (2018) Antimicrobial activity of cerium oxide nanoparticles on opportunistic microorganisms: a systematic review. Biomed Res Int 2018: 1923606

Gabrielyan L, Badalyan H, Gevorgyan V, Trchounian A (2020) Comparable antibacterial effects and action mechanisms of silver and iron oxide nanoparticles on Escherichia coli and Salmonella typhimurium. Sci Rep 10:1–12

Gharpure S, Akash A, Ankamwar B (2020) A review on antimicrobial properties of metal nanoparticles. J Nanosci Nanotechnol 20:3303–3339

Ghorbanpour M, Bhargava P, Varma A, Choudhary DK (2020) Biogenic nanoparticles and their use in agro-ecosystems. Springer, Singapore

Gudkov SV, Burmistrov DE, Serov DA, Rebezov MB, Semenova AA, Lisitsyn AB (2021) A mini review of antibacterial properties of ZnO nanoparticles. Front Phys 9:641481. https://doi.org/10.3389/fphy

Guerra JD, Sandoval G, Patron A, Avalos-Borja M, Pestryakov A, Garibo D, Susarrey-Arce A, Bogdanchikova N (2020) Selective antifungal activity of silver nanoparticles: a comparative study between Candida tropicalis and Saccharomyces boulardii. Colloid Interface Sci Commun 37:100280

Gürsoy N, Öztürk BY (2021) Synthesis of intracellular and extracellular gold nanoparticles with a green machine and its antifungal activity. Turk J Biol 45:196

Gurunathan S, Kang M-H, Qasim M, Kim J-H (2018) Nanoparticle-mediated combination therapy: two-in-one approach for cancer. Int J Mol Sci 19:3264

Gurunathan S, Qasim M, Choi Y, Do JT, Park C, Hong K, Kim JH, Song H (2020) Antiviral potential of nanoparticles-can nanoparticles fight against coronaviruses? Nanomaterials (Basel) 10:1645

Hariyadi DM, Islam N (2020) Current status of alginate in drug delivery. Adv Pharmacol Pharm Sci 2020:8886095

Hasan S (2014) A review on nanoparticles: their synthesis and types. Res J Recent Sci 2277:2502

Hashem AH, Abdelaziz AM, Askar AA, Fouda HM, Khalil A, Abd-Elsalam KA, Khaleil MM (2021) Bacillus megaterium-mediated synthesis of selenium nanoparticles and their antifungal activity against Rhizoctonia solani in faba bean plants. J Fungi 7:195

Basri HH, Talib RA, Sukor R, Othman SH, Ariffin H (2020) Effect of synthesis temperature on the size of ZnO nanoparticles derived from pineapple peel extract and antibacterial activity of ZnO-starch nanocomposite films. Nanomaterials 10:1061

Heera P, Shanmugam S (2015) Nanoparticle characterization and application: an overview. Int J Curr Microbiol App Sci 4:379–386

Hosseini SS, Joshaghani H, Shokohi T, Ahmadi A, Mehrbakhsh Z (2020) Antifungal activity of ZnO nanoparticles and Nystatin and downregulation of SAP1-3 genes expression in fluconazole-resistant Candida albicans isolates from vulvovaginal candidiasis. Infect Drug Resist 13:385

Huang T, Kumari S, Herold H, Bargel H, Aigner TB, Heath DE, O'Brien-Simpson NM, O'Connor AJ, Scheibel T (2020) Enhanced antibacterial activity of Se nanoparticles upon coating with recombinant spider silk protein eADF4 (κ16). Int J Nanomedicine 15:4275

Ibrahim H (2020) Nanotechnology and its applications to medicine: an over view. QJM Int J Med 113. https://doi.org/10.1093/qjmed/hcaa060.008

Ilaiyaraja N, Fathima SJ, Khanum F (2018) Quantum dots: a novel fluorescent probe for bioimaging and drug delivery applications. In: Inorganic frameworks as smart nanomedicines. Elsevier, pp 529–563

Irshad MA, Nawaz R, ur Rehman MZ, Imran M, Ahmad J, Ahmad S, Inam A, Razzaq A, Rizwan M, Ali S (2020) Synthesis and characterization of titanium dioxide nanoparticles by chemical and green methods and their antifungal activities against wheat rust. Chemosphere 258:127352

Javed B, Raja NI, Nadhman A (2020a) Understanding the potential of bio-fabricated non-oxidative silver nanoparticles to eradicate Leishmania and plant bacterial pathogens. Appl Nanosci 10: 2057–2067

Javed B, Nadhman A, Mashwani Z-U-R (2020b) Phytosynthesis of Ag nanoparticles from Mentha longifolia: their structural evaluation and therapeutic potential against HCT116 colon cancer, Leishmanial and bacterial cells. Appl Nanosci 10:3503–3515

Jeremiah SS, Miyakawa K, Morita T, Yamaoka Y, Ryo A (2020) Potent antiviral effect of silver nanoparticles on SARS-CoV-2. Biochem Biophys Res Commun 533:195–200

Jiao Y, Tibbits A, Gillman A, Hsiao M-S, Buskohl P, Drummy LF, Vaia RA (2018) Deformation behavior of polystyrene-grafted nanoparticle assemblies with low grafting density. Macromolecules 51:7257–7265

Jin L, Hu B, Kuddannaya S, Zhang Y, Li C, Wang ZJPC (2018) A three-dimensional carbon nanotube–nanofiber composite foam for selective adsorption of oils and organic liquids. Polym Compos 39:E271–E277

Joyce P, Ulmefors H, Maghrebi S, Subramaniam S, Wignall A, Jõemetsa S, Höök F, Prestidge CA (2020) Enhancing the cellular uptake and antibacterial activity of rifampicin through encapsulation in mesoporous silica nanoparticles. Nanomaterials 10:815

Kalagatur NK, Nirmal Ghosh OS, Sundararaj N, Mudili V (2018) Antifungal activity of chitosan nanoparticles encapsulated with Cymbopogon martinii essential oil on plant pathogenic fungi Fusarium graminearum. Front Pharmacol 9:610

Kalia A, Kaur J, Tondey M, Manchanda P, Bindra P, Alghuthaymi MA, Shami A, Abd-Elsalam KA (2021) Differential antimycotic and antioxidant potentials of chemically synthesized zinc-based nanoparticles derived from different reducing/complexing agents against pathogenic fungi of maize crop. J Fungi 7:223

Kamle M, Kumar P (2016) Colletotrichum gloeosporioides: pathogen of anthracnose disease in mango (Mangifera indica L.). In: Current trends in plant disease diagnostics and management practices. Springer, Cham, pp 207–219

Khatoon N, Mishra A, Alam H, Manzoor N, Sardar M (2015) Biosynthesis, characterization, and antifungal activity of the silver nanoparticles against pathogenic Candida species. Bionanoscience 5:65–74

Khiev D, Mohamed ZA, Vichare R, Paulson R, Bhatia S, Mohapatra S, Lobo GP, Valapala M, Kerur N, Passaglia CL (2021) Emerging nano-formulations and nanomedicines applications for ocular drug delivery. Nanomaterials 11:173

Kiseleva IV, Farroukh MA, Skomorokhova EA, Rekstin AR, Bazhenova EA, Magazenkova DN, Orlov IA, Rudenko LG, Broggini M, Puchkova LV (2020) Anti-influenza effect of nanosilver in a mouse model. Vaccine 8:679

Kumar P, Shivam P, Mandal S, Prasanna P, Kumar S, Prasad SR, Kumar A, Das P, Ali V, Singh SK (2019) Synthesis, characterization, and mechanistic studies of a gold nanoparticle–amphotericin B covalent conjugate with enhanced antileishmanial efficacy and reduced cytotoxicity. Int J Nanomedicine 14:6073

Kumar P, Mahajan P, Kaur R, Gautam S (2020) Nanotechnology and its challenges in the food sector: a review. Mater Today Chem 17:100332

Lipșa F-D, Ursu E-L, Ursu C, Ulea E, Cazacu A (2020) Evaluation of the antifungal activity of gold–chitosan and carbon nanoparticles on Fusarium oxysporum. Agronomy 10:1143

Lotfali E, Toreyhi H, Sharabiani KM, Fattahi A, Soheili A, Ghasemi R, Keymaram M, Rezaee Y, Iranpanah S (2021) Comparison of antifungal properties of gold, silver, and selenium nanoparticles against amphotericin B-resistant Candida glabrata clinical isolates. Avicenna J Med Biotechnol 13:47

Lu H, Wang J, Wang T, Zhong J, Bao Y, Hao H (2016) Recent progress on nanostructures for drug delivery applications. J Nanomater 2016. https://doi.org/10.1155/2016/5762431

Mahy M, Marsh K, Sabin K, Wanyeki I, Daher J, Ghys PD (2019) HIV estimates through 2018: data for decision-making. AIDS (London, England) 33:S203

Mba IE, Nweze EI (2020) The use of nanoparticles as alternative therapeutic agents against Candida infections: an up-to-date overview and future perspectives. World J Microbiol Biotechnol 36:1–20

Mitchell MJ, Billingsley MM, Haley RM, Wechsler ME, Peppas NA, Langer R (2020) Engineering precision nanoparticles for drug delivery. Nat Rev Drug Discov 20:1–24

Mohanraj VJ, Chen Y (2006) Nanoparticles—a review. Trop J Pharm Res 5:561–573

Mohanta YK, Biswas K, Jena SK, Hashem A, Abd-Allah EF, Mohanta TK (2020) Anti-biofilm and antibacterial activities of silver nanoparticles synthesized by the reducing activity of phytoconstituents present in the Indian medicinal plants. Front Microbiol 11. https://doi.org/10.3389/fmicb.2020.01143

Naseer M, Aslam U, Khalid B, Chen B (2020) Green route to synthesize Zinc Oxide Nanoparticles using leaf extracts of Cassia fistula and Melia azadarach and their antibacterial potential. Sci Rep 10:1–10

Nguyen VT, Dang-Thi M-S, Trinh KS (2020) Antifungal activity of Gelatin-Tapioca starch film and coating containing copper nanoparticles against Colletotrichum gloeosporioides causing anthracnose. J Chem 2020:6667450

Nunes ML, Carlini CR, Marinowic D, Neto FK, Fiori HH, Scotta MC, Zanella PLÁ, Soder RB, da Costa JC (2016) Microcephaly and Zika virus: a clinical and epidemiological analysis of the current outbreak in Brazil. J Pediatr 92:230–240

Ojea-Jimenez I, Comenge J, Garcia-Fernandez L, Megson ZA, Casals E, Puntes VF (2013) Engineered inorganic nanoparticles for drug delivery applications. Curr Drug Metab 14:518–530

Osonga FJ, Akgul A, Yazgan I, Akgul A, Eshun GB, Sakhaee L, Sadik OA (2020) Size and shape-dependent antimicrobial activities of silver and gold nanoparticles: a model study as potential fungicides. Molecules 25:2682

Pacho MN, Pugni EN, Díaz Sierra JB, Morell ML, Sepúlveda CS, Damonte EB, García CC, D'Accorso NB (2021) Antiviral activity against Zika virus of a new formulation of curcumin in poly lactic-co-glycolic acid nanoparticles. J Pharm Pharmacol 73:357–365

Pardhiya S, Paulraj R (2016) Role of nanoparticles in targeted drug delivery system. Nanotechnol Drug Deliv 2:21–51

Pariona N, Mtz-Enriquez AI, Sánchez-Rangel D, Carrión G, Paraguay-Delgado F, Rosas-Saito G (2019) Green-synthesized copper nanoparticles as a potential antifungal against plant pathogens. RSC Adv 9:18835–18843

Parvez S, Yadagiri G, Gedda MR, Singh A, Singh OP, Verma A, Sundar S, Mudavath SL (2020a) Modified solid lipid nanoparticles encapsulated with Amphotericin B and Paromomycin: an effective oral combination against experimental murine visceral leishmaniasis. Sci Rep 10:1–14

Parvez S, Yadagiri G, Karole A, Singh OP, Verma A, Sundar S, Mudavath SL (2020b) Recuperating the biopharmaceutical aspects of amphotericin B and paromomycin using a chitosan functionalized nanocarrier via oral route for enhanced anti-leishmanial activity. Front Cell Infect Microbiol 10:576

Patra JK, Das G, Fraceto LF, Campos EVR, del Pilar Rodriguez-Torres M, Acosta-Torres LS, Diaz-Torres LA, Grillo R, Swamy MK, Sharma S (2018) Nano based drug delivery systems: recent developments and future prospects. J Nanobiotechnol 16:1–33

Paul S, Mohanram K, Kannan I (2018) Antifungal activity of curcumin-silver nanoparticles against fluconazole-resistant clinical isolates of Candida species. Int Q J Res Ayurveda 39:182

Pfaller MA, Carvalhaes CG, Smith CJ, Diekema DJ, Castanheira M (2020) Bacterial and fungal pathogens isolated from patients with bloodstream infection: frequency of occurrence and antimicrobial susceptibility patterns from the SENTRY Antimicrobial Surveillance Program (2012–2017). Diagn Microbiol Infect Dis 97:115016

Piktel E, Suprewicz Ł, Depciuch J, Cieśluk M, Chmielewska S, Durnaś B, Król G, Wollny T, Deptuła P, Kochanowicz J (2020) Rod-shaped gold nanoparticles exert potent candidacidal activity and decrease the adhesion of fungal cells. Fut Med 15:2733–2752

Pilaquinga F, Morey J, Torres M, Seqqat R, de Las Nieves Piña M (2021) Silver nanoparticles as a potential treatment against SARSCoV-2: a review. Wiley Interdiscip Rev Nanomed Nanobiotechnol 77:e1707

Rahmati F, Hosseini SS, Safai SM, Lajayer BA, Hatami M (2020) New insights into the role of nanotechnology in microbial food safety. 3 Biotech 10:1–15

Rao L, Xia S, Xu W, Tian R, Yu G, Gu C, Pan P, Meng Q-F, Cai X, Qu D et al (2020) Decoy nanoparticles protect against COVID-19 by concurrently adsorbing viruses and inflammatory cytokines. J Proc Natl Acad Sci 117:27141–27147

Ray L, Karthik R, Srivastava V, Singh SP, Pant AB, Goyal N, Gupta KC (2020) Efficient antileishmanial activity of amphotericin B and piperine entrapped in enteric coated guar gum nanoparticles. Drug Deliv Transl Res 11:118–130

Rehman S, Farooq R, Jermy R, Asiri SM, Ravinayagam V, Jindan RA, Alsalem Z, Shah MA, Reshi Z, Sabit H (2020) A Wild Fomes fomentarius for biomediation of one pot synthesis of titanium oxide and silver nanoparticles for antibacterial and anticancer application. Biomol Ther 10:622

Riezk A, Van Bocxlaer K, Yardley V, Murdan S, Croft SL (2020) Activity of amphotericin B-loaded chitosan nanoparticles against experimental cutaneous leishmaniasis. Molecules 25: 4002

Riffe T, Acosta E (2021) Data resource profile: COVerAGE-DB: a global demographic database of COVID-19 cases and deaths. Int J Epidemiol 50:390–390f

Riyaz B, Sudhakar K, Mishra V (2019) Quantum dot-based drug delivery for lung cancer. In: Nanotechnology-based targeted drug delivery systems for lung cancer. Elsevier, pp 311–326

Roy S, Rhim J-W (2020) Fabrication of copper sulfide nanoparticles and limonene incorporated pullulan/carrageenan-based film with improved mechanical and antibacterial properties. Polymers 12:2665

Rozilah A, Jaafar CN, Sapuan SM, Zainol I, Ilyas RA (2020) The effects of silver nanoparticles compositions on the mechanical, physiochemical, antibacterial, and morphology properties of sugar palm starch biocomposites for antibacterial coating. Polymers 12:2605

Saleem K, Khursheed Z, Hano C, Anjum I, Anjum S (2019) Applications of nanomaterials in leishmaniasis: a focus on recent advances and challenges. Nanomaterials 9:1749

Saqib M, Ali Bhatti AS, Ahmad NM, Ahmed N, Shahnaz G, Lebaz N, Elaissari A (2020) Amphotericin B loaded polymeric nanoparticles for treatment of leishmania infections. Nanomaterials 10:1152

Sattary M, Amini J, Hallaj R (2020) Antifungal activity of the lemongrass and clove oil encapsulated in mesoporous silica nanoparticles against wheat's take-all disease. Pestic Biochem Physiol 170:104696

Sepulveda AAL, Velasquez AMA, Linares IAPO, de Almeida L, Fontana CR, Garcia C, Graminha MAS (2020) Efficacy of photodynamic therapy using TiO2 nanoparticles doped with Zn and hypericin in the treatment of cutaneous leishmaniasis caused by Leishmania amazonensis. Photodiagn Photodyn Ther 30:101676

Shakibaie M, Mohazab NS, Mousavi SAA (2015) Antifungal activity of selenium nanoparticles synthesized by Bacillus species Msh-1 against Aspergillus fumigatus and Candida albicans. Jundishpur J Microbiol 8:e26381

Shende S, Bhagat R, Raut R, Rai M, Gade A (2021) Myco-fabrication of copper nanoparticles and its effect on crop pathogenic fungi. IEEE Trans Nanobioscience 20:146–153

Silva Viana RL, Pereira Fidelis G, Medeiros MJC, Morgano MA, Alves MGCF, Passero LFD, Pontes DL, Theodoro RC, Arantes TD, Sabry DA (2020) Green synthesis of antileishmanial and antifungal silver nanoparticles using corn cob xylan as a reducing and stabilizing agent. Biomol Ther 10:1235

Singh K, Garg G, Ali V (2016) Current therapeutics, their problems and thiol metabolism as potential drug targets in leishmaniasis. Curr Drug Metab 17:897–919

Skinder BM, Hamid S (2020) Nanotechnology: a modern technique for pollution abatement. In: Bioremediation and biotechnology, vol 4. Springer, Cham, pp 295–311

Slavin YN, Asnis J, Häfeli UO, Bach H (2017) Metal nanoparticles: understanding the mechanisms behind antibacterial activity. J Nanobiotechnol 15:1–20

Sudha PN, Sangeetha K, Vijayalakshmi K, Barhoum A (2016) Nanomaterials history, classification, unique properties, production and market. In: Emerging applications of nanoparticles and architecture nanostructures. Elsevier, pp 341–384

Sun Y, Yin Y, Gong L, Liang Z, Zhu C, Ren C, Zheng N, Zhang Q, Liu H, Liu W (2021) Manganese nanodepot augments host immune response against coronavirus. Nano Res 14: 1260–1272

Surnar B, Kamran MZ, Shah AS, Dhar S (2020) Clinically approved antiviral drug in an orally administrable nanoparticle for COVID-19. ACS Pharmacol Transl Sci 3:1371–1380

Szunerits S, Barras A, Khanal M, Pagneux Q, Boukherroub R (2015) Nanostructures for the inhibition of viral infections. Molecules 20:14051–14081

Thangadurai D, Sangeetha J, Prasad R (2020) Nanotechnology for food, agriculture, and environment. Springer, Cham

Varahachalam SP, Lahooti B, Chamaneh M, Bagchi S, Chhibber T, Morris K, Bolanos JF, Kim N-Y, Kaushik A (2021) Nanomedicine for the SARS-CoV-2: state-of-the-art and future prospects. Int J Nanomedicine 16:539

Wall G, Lopez-Ribot JL (2020) Current antimycotics, new prospects, and future approaches to antifungal therapy. Antibiotics 9:445

Wang CY, Makvandi P, Zare EN, Tay FR, Niu LN (2020) Advances in antimicrobial organic and inorganic nanocompounds in biomedicine. Adv Therap 3:2000024

Wang C, Wang S, Chen Y, Zhao J, Han S, Zhao G, Kang J, Liu Y, Wang L, Wang X (2021) Membrane nanoparticles derived from ACE2-rich cells block SARS-CoV-2 infection. ACS Nano 15:6340–6351

Wilczewska AZ, Niemirowicz K, Markiewicz KH, Car H (2012) Nanoparticles as drug delivery systems. Pharmacol Rep 64:1020–1037

World Health Organization (2021) 2020 Antibacterial agents in clinical and preclinical development: an overview and analysis. Available at: https://www.who.int/publications/i/item/9789240021303. Accessed 5 May 2021

Xing H, Hwang K, Lu Y (2016) Recent developments of liposomes as nanocarriers for theranostic applications. Theranostics 6:1336

Yadav D, Sandeep K, Pandey D, Dutta RK (2017) Liposomes for drug delivery. J Biotechnol Biomater 7:276

Yetisgin AA, Cetinel S, Zuvin M, Kosar A, Kutlu O (2020) Therapeutic nanoparticles and their targeted delivery applications. Molecules 25:2193